T. Alexander, P. Natarajan, Science, 7 August 2014 (10.1126/science.1251053).

# Rapid growth of seed black holes in the early universe by supra-exponential accretion

Tal Alexander,[1⋆] Priyamvada Natarajan[2]

[1]Department of Particle Physics & Astrophysics, Weizmann Institute of Science, Rehovot 76100, Israel

[2]Department of Astronomy, Yale University, 260 Whitney Avenue, New Haven, CT 06511, USA

⋆Corresponding author. E-mail: tal.alexander@weizmann.ac.il

**Mass accretion by black holes (BHs) is typically capped at the Eddington rate, when radiation's push balances gravity's pull. However, even exponential growth at the Eddington-limited $e$-folding time $t_E \sim \mathrm{few}\times 0.01$ billion years, is too slow to grow stellar-mass BH seeds into the supermassive luminous quasars that are observed when the universe is $1$ billion years old. We propose a dynamical mechanism that can trigger supra-exponential accretion in the early universe, when a BH seed is bound in a star cluster fed by the ubiquitous dense cold gas flows. The high gas opacity traps the accretion radiation, while the low-mass BH's random motions suppress the formation of a slowly-draining accretion disk. Supra-exponential growth can thus explain the puzzling emergence of supermassive BHs that power luminous quasars so soon after the Big Bang.**

Optically bright quasars powered by accretion onto black holes (BHs) are now detected at redshifts as high as $z \sim 7$, when the Universe was 6% of its current age ($< 1$ billion years) (*1*). Their luminosities imply supermassive BHs (SMBHs) with the mass of the BH ($M_\bullet$) $\gtrsim 10^9$ solar masses ($M_\odot$) (*2*). The main obstacles to assembling such SMBHs so rapidly are the low masses of the hypothesized initial seed BHs, born of first-generation (Pop III) stars, coupled with the maximal growth rate for radiatively efficient accretion, the Eddington limit (*3, 4, 5*). Proposed ways to circumvent these limitations invoke super-Eddington accretion for brief periods of time (*6*); the *ab-initio* formation of more massive BH seeds (*7, 8, 9, 10*) from the direct collapse of self-gravitating pre-galactic gas disks at high redshifts (*11, 12, 13, 14*); and the formation of a very massive star from runaway stellar mergers in a dense cluster (*15, 16*). Discriminating between these scenarios is challenging, because seed formation redshifts ($z > 10$) are observationally inaccessible. Current data require finely tuned, continuous early BH growth and massive initial BH seeds (*17, 18, 19, 20*). Recent results from high-resolution simulations of early star formation at $z \sim 15$ to $18$ exacerbate the problem by indicating that efficient fragmentation and turbulence (*21, 22, 23, 24, 25*) lead to the efficient formation of stellar clusters

embedded in the flow, which prevents the formation of massive seeds ($\gg 10\,M_\odot$) by limiting the mass of their potential Pop III progenitor stars. On the other hand, theoretical and numerical results on larger scales suggest that ubiquitous dense cold gas flows (*26*) stream in along filaments and feed proto-galactic cores (*27, 28*). Adaptive mesh refinement simulations track the fate of these sites (collapsed $10^7\,M_\odot$ dark matter halos) from $1\,\mathrm{Mpc}$ scale at $z\sim 21$ with resolutions as low as $\sim 2\times 10^{-10}$ pc in the central regions. These simulations find isothermal density cusps that reach extreme central densities, with an average density of $\rho_\infty \gtrsim 10^{-16}\,\mathrm{g\,cm^{-3}}$ ($\gtrsim 10^8\,\mathrm{cm^{-3}}$ for pure H) on $0.1$ pc scales (*29*). They also reveal a marginally unstable central gas reservoir of $\mathrm{few}\times 10^5\,M_\odot$ in the inner few parsecs (*30*) , where the dynamical timescale is $\sim 10^6$ years. Although these simulations are somewhat idealized, we adopt the properties of this high density environment as the initial conditions for the model presented here.

We consider a scenario in which a low-mass Pop III remnant BH remains embedded in a nuclear star cluster fed by dense cold gas flows (*26*) (Figure 1 and Table 1). The stars and gas are virialized in the cluster potential, and the BH is initially a test particle in equipartition with the stars. Gas within the accretion (capture) radius of the BH, $r_a = [2c^2/(c_\infty^2+v_\bullet^2)]r_g$, is dynamically bound to it, where $r_g = GM_\bullet/c^2$ is the gravitational radius of the BH; $c_\infty$ is the gas sound speed in the cold flow far from the BH, which is a measure of the depth of the cluster's gravitational potential; and $v_\bullet$ is the BH velocity relative to the gas. Gas bound to the BH inside $r_a$ is not necessarily accreted by it. Prompt accretion requires gas to flow from $r_a$ into the BH on a plunging trajectory with low specific angular momentum $j < j_{\rm ISO} \simeq 4r_g c$, through the innermost stable periapse distance $r_{\rm ISO}$. It is this angular momentum barrier, rather than the Eddington limit, that is the main obstacle to supra-exponential growth.

The BH is more massive than a cluster star, so $v_\bullet^2 < c_\infty^2$, and the accretion flow is quasi-spherical. In the idealized case where the flow is radial and adiabatic, it is described by the Bondi solution (*31*), $\dot{M}_B = (\pi/\sqrt{2})r_a^2\rho_\infty c_\infty$ (adiabatic index $\Gamma = 4/3$ assumed), which can be written compactly in terms of $\mu = M_\bullet/M_i$, where $M_i$ is the initial BH mass, as $\dot{\mu} = \mu^2/t_B$, with timescale $t_B = c_\infty^3\,/2^{3/2}\pi G^2 M_i\rho_\infty$. The stronger-than-linear dependence of the accretion rate on the BH mass leads to a solution that diverges supra-exponentially in a finite time $t_B$ as $\mu(t) = 1/(1-t/t_B)$. Physical flows, where gravitational energy is released as radiation, are not strictly adiabatic. As the mass accretion rate grows, the local luminosity can far exceed the Eddington luminosity $L_E = 4\pi cGM_\bullet/\kappa = \dot{M}_E c^2$ ($\kappa$ is the gas opacity), for which radiation flux pressure balances gravity. However, radiation produced inside the photon-trapping radius $r_\gamma \sim (\dot{M}/\dot{M}_E)r_g$ is carried with the flow into the BH, because the local optical depth $\tau(r)\sim\kappa\rho(r)r$ makes photon diffusion outward slower than accretion inward (*32*) [which is a manifestation of the $\mathcal{O}(v/c)$ effect of relativistic beaming (*33*)]. The luminosity $L_\infty$ that escapes to infinity from $r \gtrsim r_\gamma$ translates to a lowered radiative efficiency $\eta_\gamma = L_\infty/\dot{M}c^2 \sim \min(r_g/r_\gamma, r_g/r_{\rm ISO})$, so it does not exceed $\sim L_E$, thereby allowing supra-exponential Bondi mass accretion rates (*34*). Detailed calculations show that $L_\infty \lesssim 0.6L_E$ (*35*). The associated radiation pressure enters the dynamics of the flow as an effective reduction of gravity by a factor $0.4$, and consequently, as a reduction of the accretion rate by $0.4^2 \simeq 1/6$. The supra-exponential divergence of spherical

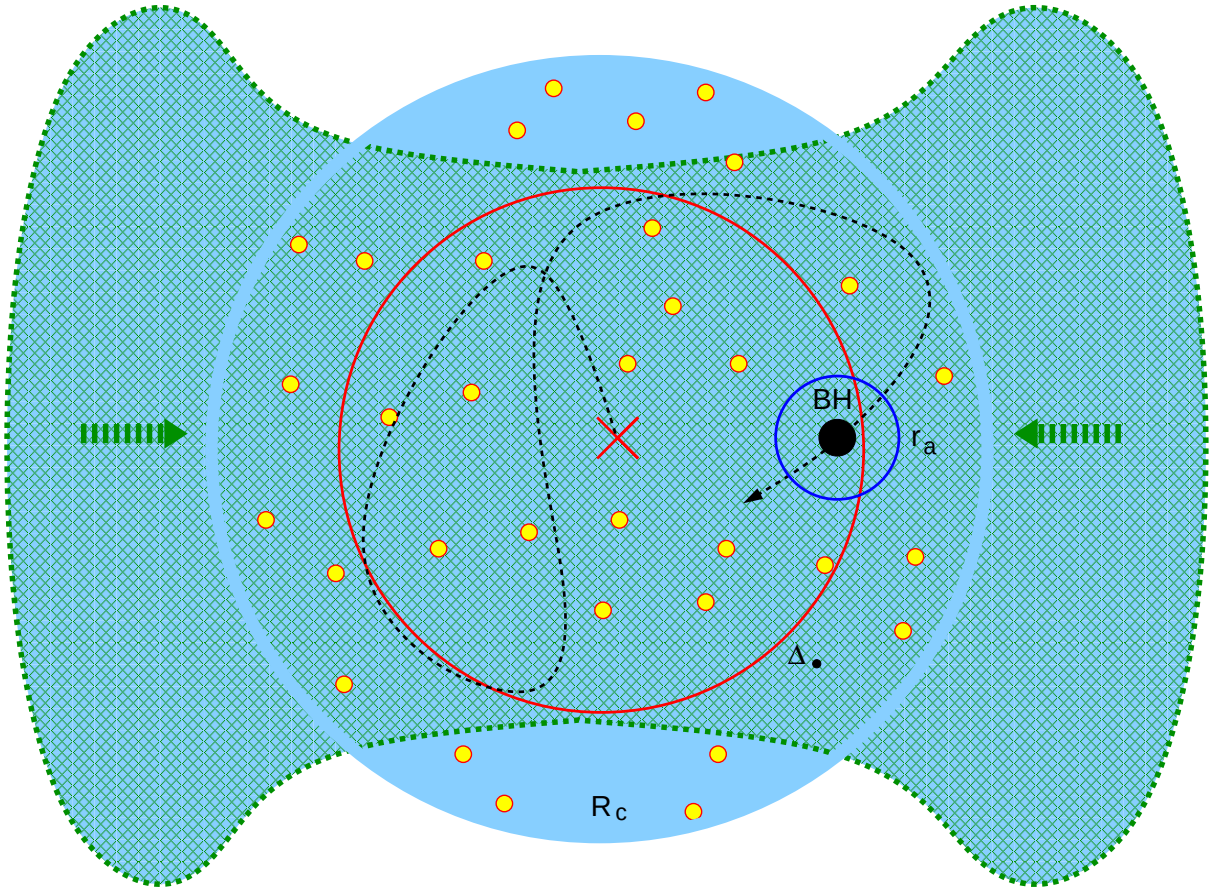


Figure 1: A schematic depiction of accretion by a low-mass BH in a dense gas-rich cluster. Dense cold gas (green) flows to the center (red cross) of a stellar cluster (light blue region) of total mass $M_c = N_\star M_\star + M_g$ and radius $R_c$, which contains $N_\star$ stars (yellow circles) of mass $M_\star$ each with velocity dispersion $\sigma_\star$, and gas of mass $M_g$. The gas is nearly pressure-supported and close to the virial temperature. A stellar BH (black circle) of mass $M_\star < M_\bullet \ll M_c$, which is accreting from its capture radius $r_a$ (dark blue circle), is initially in fluctuation-dissipation equilibrium with the stars and is scattered by them (black dashed line) with velocity dispersion $\sigma_\bullet \sim \sqrt{M_\star/M_\bullet}\sigma_\star$ over a distance scale $\Delta_\bullet \sim \sqrt{M_\star/M_\bullet}R_c$ (red circle).

accretion is therefore

$$M_\bullet(t) = \frac{M_i}{1 - t/t_\infty}\,, \;\; t_\infty \simeq 6t_B = \frac{3}{2^{1/2}\pi}\frac{c_\infty^3}{G^2 M_i \rho_\infty}\,. \tag{1}$$

The typical lifetime of cold flow streams seen in simulations is $\gtrsim 10^7$ years (*29*), which is long enough for the $\sim 10^5\,M_\odot$ of gas in the marginally unstable reservoir on the few parsec scale to accrete onto the growing BH, and yet short enough to be relevant for forming $z > 7$ quasars. As a demonstration of concept, we adopt the gas properties found in these simulations, and match a divergence time of $t_\infty \sim \mathrm{few}\times 10^7$ years to the mean physical parameters of the $4 \times 10^4\,M_\odot$ of gas on the $0.25$-pc scale. We further assume that half of that mass is in a star cluster with $1\,M_\odot$ stars in a nonsingular distribution (a Plummer law), containing a $10\,M_\odot$ stellar BH, and that the escaped radiation from $r > r_\gamma$ does not substantially affect the cold flow on larger scales. This cluster, while dense, is dynamically stable on timescales $\gg t_\infty$. Table 1 lists the input physical parameters of the model, the derived gas and cluster properties, and the predicted accretion properties.

Simulations (*29*) find that the cold flow is nearly pressure-supported, and thus has little angular momentum. It is also plausible that there is little net rotation between the gas and the stars that were formed from it. However, unavoidable gravitational interactions of the low-mass BH with cluster stars accelerate it at orbital frequencies of $\Omega(r_\bullet) \sim \Omega_0$, which induce a velocity gradient across the capture radius. Gas captured by the BH then acquires specific angular momentum relative to it, $j_a$, due to the opposite velocity and density gradients and the velocity-skewed capture cross-section ($j_{a,v} \sim \Omega r_a^2$ and $j_{a,\rho} \sim (\mathrm{d}\log\rho/\mathrm{d}\log r)_{r_\bullet}\Omega r_a^2$) (*36*). Gas with $j_a > j_{\rm ISO}$ cannot plunge directly into the BH but rather circularizes at a radius $r_c = j_a^2/GM_\bullet$, and accretion then proceeds on the slow viscous timescale rather than the fast, near-free fall timescale. Analytic and numeric results on the capture efficiency of angular momentum by inhomogeneous wind accretion are currently available only in the ballistic (supersonic) limit (*37*, *38*). We adapt these results to provide a rough estimate of the angular momentum in the accretion flow on the BH seed in the subsonic regime considered here (see details in the Supplementary Materials).

The formal divergence of $j_a/j_{\rm ISO} \propto M_\bullet$ in the test particle limit, where $\Omega \sim \Omega_0$, is reversed by the accretion itself. The nonrotating gas accreted by the BH from the cluster exerts a drag on it, $\ddot{\boldsymbol{r}}_\bullet = -2\gamma_a\dot{\boldsymbol{r}}_\bullet$, where $\gamma_a = \dot{M}/2M_\bullet = M_\bullet(t)/2M_i t_\infty$. This provides additional damping beyond dissipation by dynamical friction against the gas and stars, $\gamma_{\rm df} \propto [M_\bullet(t)/M_c]\Omega_0$ (*39*), which is balanced by the two-body fluctuations. Accretion damping drives the BH to sub-equipartition energy and angular momentum. Two-body interactions with the cluster stars can reestablish equipartition on the central relaxation timescale $t_{r0} \sim 2 \times 10^7$ years only as long as the BH growth rate $2\gamma_a$ is slower than the relaxation rate, up to time $t_{\rm eq}/t_\infty = 1 - t_{r0}/t_\infty \sim 0.6$ (Eq. 1), when the BH has grown by a factor of only $t_\infty/t_{r0} \sim 2.5$ to $M_{\rm eq} \simeq 25\,M_\odot$. At later times, $j_a$ is expected to fall below the extrapolated test particle limit, because both the BH wandering radius $\Delta_\bullet$ and the orbital frequency $\Omega$ are increasingly damped by dynamical friction and by the accretion drag, which are both $\propto M_\bullet(t)$.

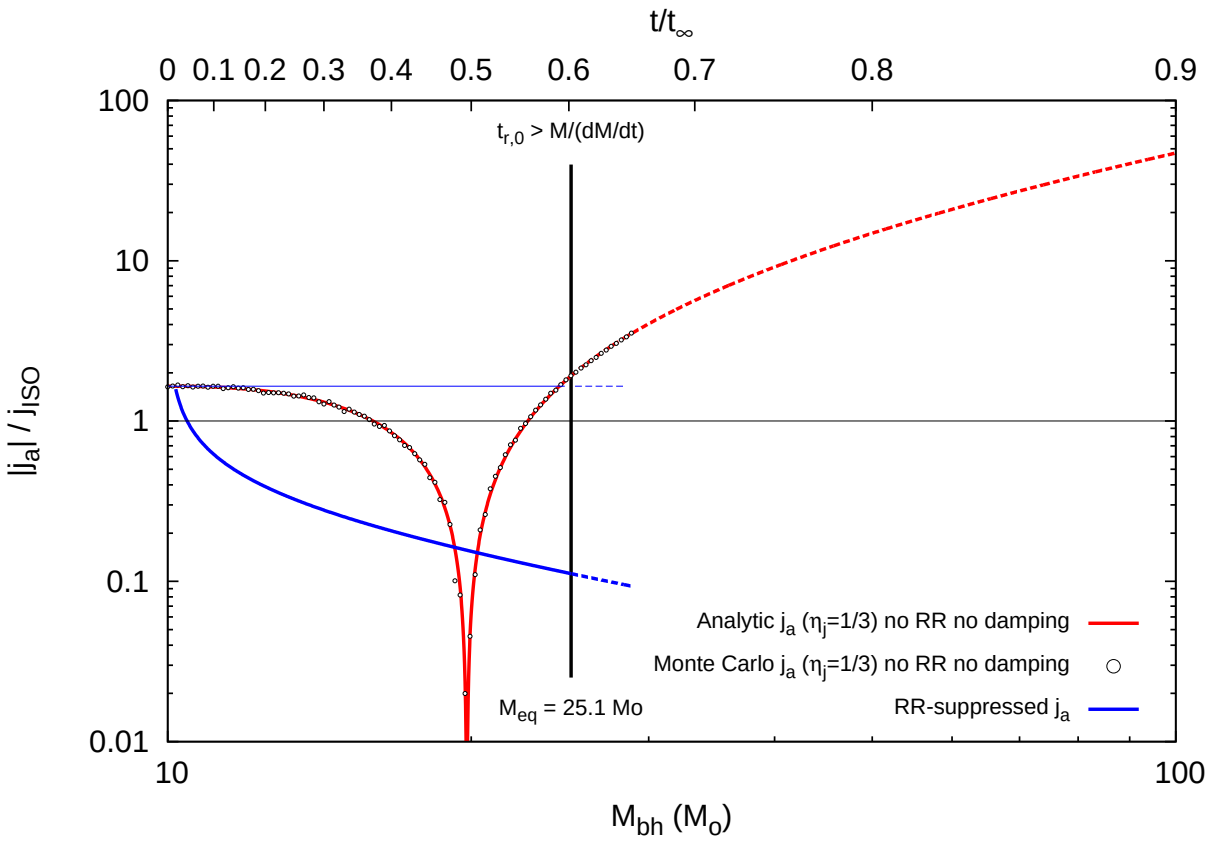


Figure 2: The specific angular momentum ratio, $j_a/j_{\rm ISO}$, in gas captured by the BH, as function of the BH mass $M_\bullet$ (and the corresponding $t/t_\infty$ for Bondi accretion). The evolution of $j_a/j_{\rm ISO}$ during the initial stages of the BH growth is calculated in the ballistic wind accretion limit by a first-order analytic estimate with an angular momentum capture efficiency of $\eta_j = 1/3$ (red line), which is validated against results from a Monte Carlo integration over the exact capture cross-section (circles). $j_a$ falls to zero at $M_0 \simeq 20\,M_\odot$, where the density and velocity gradients cancel each other. The vertical line at $M_{\rm eq} \simeq 25\,M_\odot$ marks the transition to a dynamical regime where two-body relaxation can no longer establish equipartition between the growing BH and the stars, and the acceleration frequency $\Omega$ is damped. The early dynamical suppression of the angular momentum down to $j_a < j_{\rm ISO}$ by resonant relaxation of the BH orbit (thick blue line) is approximated by conservatively assuming a constant $j_a(t) = j_a(0)$ (thin blue line). At $M_\bullet > M_{\rm eq}$, where the BH dynamics are sub-equipartition, the actual value of $j_a/j_{\rm ISO}$ is expected to progressively drop below the extrapolated one (dashed lines). (See the detailed discussion in the Supplementary Materials).

Table 1: Supra-exponential BH growth model

| **Property**$^\star$ | **Notation** | **Value** |
|---|---|---|
| *Model parameters* | | |
| Initial BH mass | $M_\bullet$ | $10\,M_\odot$ |
| Star mass | $M_\star$ | $1\,M_\odot$ |
| Core radius | $R_c$ | $0.25\,\mathrm{pc}$ |
| Stellar core mass | $M_s$ | $2\times10^4\,M_\odot$ |
| Gas mass in core | $M_g$ | $2\times10^4\,M_\odot$ |
| Total core mass | $M_c$ | $4\times10^4\,M_\odot$ |
| Cold flow adiabatic index | $\Gamma$ | $5/3$ |
| *Derived cluster properties* | | |
| Mean gas density | $\rho_\infty$ | $2.1\times10^{-17}\,\mathrm{g\,cm^{-3}}$ |
| Jeans sound speed | $c_s$ | $14.5\,\mathrm{km\,s^{-1}}$ |
| Velocity dispersion | $\sigma_\star$ | $18.0\,\mathrm{km\,s^{-1}}$ |
| Initial BH rms velocity | $v_\bullet$ | $11.4\,\mathrm{km\,s^{-1}}$ |
| Initial BH rms scattering distance | $\Delta_\bullet$ | $6.5\times10^{-2}\,\mathrm{pc}$ |
| Cluster orbital frequency | $\Omega_0$ | $1/5545\,\mathrm{year^{-1}}$ |
| Central 2-body relaxation time | $t_{r0}$ | $1.4\times10^7\,\mathrm{years}$ |
| Vector resonant relaxation time | $t_{vRR}$ | $6.2\times10^5\,\mathrm{years}$ |
| Evaporation time | $t_{\rm evap}$ | $8.0\times10^9\,\mathrm{years}$ |
| Collisional destruction time | $t_{\rm coll}$ | $1.5\times10^{11}\,\mathrm{years}$ |
| Gas reservoir dynamical time | $t_{\rm res}$ | $\sim10^6\,\mathrm{years}$ |
| *Predicted accretion properties* | | |
| Initial accretion radius | $r_a^0$ | $2.5\times10^{-4}\,\mathrm{pc}$ |
| Mass divergence time | $t_\infty$ | $3.5\times10^7\,\mathrm{years}$ |
| Initial specific accretion ang. mom. | $j_a/j_{\rm ISO}$ | $1.6$ |
| Ang. mom. suppression by resonant relaxation | $\sqrt{t_\infty/t_{vRR}}$ | $7.6$ |

$^\star$ See also definitions and discussion in the Supplementary Materials.

Figure (2) shows the evolution of $j_a/j_{\rm ISO}$ with $M_\bullet$ for the cold flow cluster model of table (1). A key property of acceleration-induced angular momentum accretion is the existence of a BH mass scale $M_0$ where $j_a(M_0)\to 0$ on typical orbits, because the density and velocity gradients cancel each other. For a cluster in dynamic equipartition and pressure-supported gas, $M_0$ depends weakly only on the shape of the density/potential cluster model near the origin: For the Plummer model, $M_0\simeq 20M_\star$. This low mass scale is significant because $M_i<M_0<M_{\rm eq}$, and therefore $j_a/j_{\rm ISO}$ remains low during the critical stage of early growth, before damping can become effective.

In addition, vector resonant relaxation (*40, 41*), a rapid process of angular momentum relaxation that operates in nearly spherical potentials, further suppresses the growth of $j_a$ by

randomizing the BH's orbital orientation on a timescale (*42*) $t_{vRR} \sim 6 \times 10^5$ years. This decreases $j_a$ by a factor of $\sqrt{t_\infty/t_{vRR}} \sim 8$ over the divergence time. Randomization by resonant relaxation can be effective until time $t_{\rm rnd}/t_\infty = 1 - t_{vRR}/t_\infty \sim 0.98$. By that time, the BH has grown by a factor of $t_\infty/t_{vRR} \sim 60$ to $M_{\rm rnd} \simeq 600\,M_\odot$ and $> 0.95$ of its mass has been accreted from low-angular momentum gas in the absence of efficient equipartition. The effect of resonant relaxation can be estimated analytically in the early growth stages, up to $M_\bullet \sim M_{\rm eq}$, when both the growth rate and $j_a$ can be approximated as near-constant: Dynamical randomization quickly pushes $j_a/j_{\rm ISO}$ below 1 (independently of the decrease in $j_a/j_{\rm ISO}$ near $M_\bullet = M_0$) (Fig. 2). The damped and randomized motions of the BH suppress the accumulation of angular momentum in the accretion flow and allow Bondi accretion to proceed supra-exponentially.

The BH mass up to $t_{\rm rnd}$, $M_\bullet \leq M_{\rm rnd} \sim 0.02 M_c$ is still small enough to justify both treating the BH as a test particle in the fixed potential of the gas and star cluster and representing cluster dynamics by a simple model. It is much more difficult to self-consistently predict the subsequent joint evolution of the BH and cluster. However, the physical arguments for the gradual deceleration of the BH and the decline of $j_a$ beyond $M_{\rm eq} \sim 25\,M_\odot$, suggest that a substantial fraction of the available $10^5\,M_\odot$ gas reservoir can be accreted in $t_\infty \sim {\rm few}\times 10^7$ years at $z > 15$. Even if the supra-exponential growth phase terminates with a modest BH seed of only $M_{\rm rnd} = 600\,M_\odot$ at $z = 16$ ($t \simeq 0.25$ billion years for $H_0 = 0.7$, $\Omega = 1$, $\Omega_M = 0.28$), this would allow the subsequent Eddington-limited growth (with radiative efficiency $\eta_\gamma = 0.1$ and electron-scattering opacity $\kappa = 0.35\,{\rm cm^2\,g^{-1}}$) of a $3.4 \times 10^8\,M_\odot$ SMBH by $z = 7$ ($t \simeq 0.78$ billion years), and a $2.5 \times 10^{10}\,M_\odot$ one by $z = 6$ ($t \simeq 0.95$ billion years). Even if the process operates efficiently only in 1 to 5% of the dark matter halos where the first stars form, it can adequately account for the SMBHs seen to be powering the detected luminous quasars at $z > 6$.

We conclude that low mass stellar BHs in very dense, low-angular momentum cold flows at redshifts $z > 15$ can be launched by stellar dynamical processes into a phase of supply-limited, supra-exponential accretion and can grow rapidly in $\sim {\rm few}\times 10^7$ years into $\gtrsim 10^4\,M_\odot$ BH seeds. Subsequent slower Eddington-limited growth by disk accretion suffices to produce the supermassive BHs that power the brightest early quasars.

# References and Notes

1. D. J. Mortlock, *et al.*, *Nature* **474**, 616 (2011).

2. X. Fan, *et al.*, *AJ* **131**, 1203 (2006).

3. M. Jeon, *et al.*, *ApJ* **754**, 34 (2012).

4. M. Milosavljević, V. Bromm, S. M. Couch, S. P. Oh, *ApJ* **698**, 766 (2009).

5. K. Park, M. Ricotti, *ApJ* **747**, 9 (2012).

6. M. Volonteri, M. J. Rees, *ApJ* **633**, 624 (2005).

7. P. F. Hopkins, *et al.*, *ApJ* **662**, 110 (2007).

8. M. Volonteri, *A&A Rev.* **18**, 279 (2010).

9. P. Natarajan, *Bulletin of the Astronomical Society of India* **39**, 145 (2011).

10. Z. Haiman, *Astrophysics and Space Science Library*, T. Wiklind, B. Mobasher, V. Bromm, eds. (2013), vol. 396 of *Astrophysics and Space Science Library*, pp. 293–341.

11. V. Bromm, A. Loeb, *ApJ* **596**, 34 (2003).

12. G. Lodato, P. Natarajan, *MNRAS* **371**, 1813 (2006).

13. M. C. Begelman, M. Volonteri, M. J. Rees, *MNRAS* **370**, 289 (2006).

14. G. Lodato, J. E. Pringle, *MNRAS* **381**, 1287 (2007).

15. B. Devecchi, M. Volonteri, *ApJ* **694**, 302 (2009).

16. M. B. Davies, M. C. Miller, J. M. Bellovary, *ApJ* **740**, L42 (2011).

17. C. J. Willott, R. J. McLure, M. J. Jarvis, *ApJ* **587**, L15 (2003).

18. A. Ferrara, F. Haardt, R. Salvaterra, *MNRAS* **434**, 2600 (2013).

19. J. L. Johnson, D. J. Whalen, H. Li, D. E. Holz, *ApJ* **771**, 116 (2013).

20. E. Treister, K. Schawinski, M. Volonteri, P. Natarajan, *ApJ* **778**, 130 (2013).

21. M. A. Alvarez, J. H. Wise, T. Abel, *ApJ* **701**, L133 (2009).

22. T. H. Greif, *et al.*, *ApJ* **737**, 75 (2011).

23. M. J. Turk, J. S. Oishi, T. Abel, G. L. Bryan, *ApJ* **745**, 154 (2012).

24. J. A. Regan, P. H. Johansson, M. G. Haehnelt, *MNRAS* **439**, 1160 (2014).

25. C. Safranek-Shrader, M. Milosavljević, V. Bromm, *MNRAS* **440**, L76 (2014).

26. A. Dekel, *et al.*, *Nature* **457**, 451 (2009).

27. Y. Dubois, *et al.*, *MNRAS* **423**, 3616 (2012).

28. F. Bournaud, *et al.*, *ApJ* **741**, L33 (2011).

29. J. H. Wise, M. J. Turk, T. Abel, *ApJ* **682**, 745 (2008).

30. The near-stability of such a massive reservoir may require suppression of $H_2$ cooling by strong sources of Lyman-Werner radiation, implying that such reservoirs are rare. Neither effect was included explicitly in the simulations; however they have been investigated theoretically in detail [for example, (*43*)].

31. H. Bondi, *MNRAS* **112**, 195 (1952).

32. M. C. Begelman, *MNRAS* **184**, 53 (1978).

33. D. Mihalas, B. W. Mihalas, *Foundations of radiation hydrodynamics* (1984).

34. M. H. Soffel, *A&A* **116**, 111 (1982).

35. M. C. Begelman, *MNRAS* **187**, 237 (1979).

36. M. Ruffert, U. Anzer, *A&A* **295**, 108 (1995).

37. M. Livio, N. Soker, M. de Kool, G. J. Savonije, *MNRAS* **222**, 235 (1986).

38. M. Ruffert, *A&A* **346**, 861 (1999).

39. J. Binney, S. Tremaine, *Galactic Dynamics: Second Edition* (Princeton University Press, 2008).

40. K. P. Rauch, S. Tremaine, *New Astronomy* **1**, 149 (1996).

41. C. Hopman, T. Alexander, *ApJ* **645**, 1152 (2006).

42. Similar randomization by two-body relaxation is negligibly slow, by comparison. However, both two-body relaxation and resonant relaxation will be substantially accelerated by a realistic stellar mass spectrum, and inhomogeneities in the gas flow will also contribute to the randomization of the BH orbit.

43. B. Agarwal, A. J. Davis, S. Khochfar, P. Natarajan, J. S. Dunlop, *MNRAS* **432**, 3438 (2013).

## Acknowledgments

We thank P. Armitage, B. Bar-Or, M. Begelman, F. Bournaud, M. Colpi, A. Dekel. J.-P. Lasota, C. Reynolds and N. Sapir for helpful discussions and comments. T.A. acknowledges support by European Research Council Starting Grant No. 202996, DIP-BMBF Grant No. 71-0460-0101, and the I-CORE Program of the PBC and Israel Science Fund (Center No. 1829/12). P.N. acknowledges support from a NASA-NSF Theoretical and Computational Astrophysics Networks award number 1332858. The authors thank the Kavli Institute for Theoretical Physics, UC Santa Barbara, where this work was initiated and supported in part by NSF Grant PHY11-2591. T.A. is grateful for the warm hospitality of Angel Millán and Lucy Arkwright of La Posada San Marcos, Alájar, Spain, who hosted the Alájar Workshop where this work was continued.

T. Alexander, P. Natarajan, Science, 7 August 2014 (10.1126/science.1251053).

# Supplementary Materials for

# Rapid Growth of Seed Black Holes in the Early Universe by Supra-Exponential Accretion

Tal Alexander[1] and Priyamvada Natarajan[2]

[1]Department of Particle Physics & Astrophysics, Weizmann Institute of Science, Rehovot 76100, Israel

[2]Department of Astronomy, Yale University, 260 Whitney Avenue, New Haven, CT 06511, USA

correspondence to: tal.alexander@weizmann.ac.il

**This PDF file includes:**

# Supplementary Text

The supra-exponential accretion scenario for the growth of black hole (BH) seeds in the early universe ties together processes related to the stellar dynamics of the cluster with those related to the accretion flow on the BH. These are discussed in this context and derived here in detail: the dynamics of the BH in the star cluster in section S1, and the angular momentum of the accretion flow in section S2.

## S1 BH dynamics in the host cluster

The dynamical evolution of the gas-rich host stellar cluster, and the dynamics of the BH in it, can affect the nature of the accretion flow onto the BH, and the time available for the BH growth. The initial low-mass BH rapidly reaches a dynamical fluctuation / dissipation equilibrium with the stars in the dense cluster via two-body interactions. If the stellar velocities are Maxwellian, the equilibrium is that of equipartition. For the Plummer density model (*44*) that is assumed here for quantitative estimates[1], equipartition is a good approximation (*45*).

We simplify here the qualitative discussion of the dynamics by approximating the mass distribution of the nuclear star cluster as a constant density spherical core of radius $R_c$ with mass $M_c$ in stars and gas, and the velocity distribution as Maxwellian with 1D velocity dispersion $\sigma_\star$. The cluster contains $N_\star$ stars of mass $M_\star$ each (the total stellar mass in the core is $M_s = N_\star M_\star \equiv sM_c$, where $s \leq 1$), and one BH of mass $M_\bullet$. We further assume that $M_s/M_g \sim \mathcal{O}(1)$ ($s \sim 1/2$) in the core, and therefore the stellar dynamics can be approximated, to within order unity corrections, by neglecting the gas. Conversely, since the cold flows provide an effectively infinite reservoir of gas compared to $M_c$, we assume that the gas properties are not substantially affected by the stellar dynamics.

We denote the mass ratio $Q = M_\bullet/M_\star$, the core velocity $V_c^2 = GM_c/R_c$ and the core orbital frequency $\Omega_c^2 = R_c^3/GM_c$. In equipartition, the mean energy of the BH is $E_\bullet = 3M_\star\sigma_\star^2$, and therefore the BH's rms 3D velocity is $v_\bullet^2 = 3\sigma_\bullet^2 = (3/Q)\sigma_\star^2$ and its rms 3D displacement from the center is $\Delta_\bullet^2 = (3/Q)\sigma_\star^2/\Omega_c^2$. Since $\sigma_\star^2 \sim V_c^2$, it then follows that $v_\bullet^2 \sim V_c^2/Q$ and $\Delta_\bullet^2 \sim R_c^2/Q$ that is, the BH's typical velocity is significantly smaller than the typical velocity of stars in the cluster's potential, and its excursions away from the center are confined to the central regions of the core, where the density is nearly constant. An exact treatment of the fluctuation/dissipation equilibrium in the Plummer potential (*45*) yields

$$v_\bullet^2 = (2^{5/2}/3)V_c^2/Q\,, \;\; \Delta_\bullet^2 = (2/3)R_c^2/Q. \tag{S1}$$

Two-body scattering by the cluster stars changes the BH's orbital energy and angular mo-

[1]Define $M_{\rm tot} = 2^{3/2}M_c$, $x = r/R_c$, and $y = \sqrt{1+x^2}$. The Plummer density profile is $\rho = (3M_{\rm tot}/4\pi R_c^3)/y^5$, the enclosed mass is $M_< = M_{\rm tot}x^3/y^3$, the potential is $\phi = -(GM_{\rm tot}/R_c)/y$, the 1D velocity dispersion is $\sigma^2 = -\phi/6$, the fundamental frequency is $\Omega_0^2 = GM_{\rm tot}/R_c^3$, and the azimuthal velocity is $v_\phi^2 = (GM_{\rm tot}/R_c)x^2/y^3$.

mentum by order unity around their equipartition values on the relaxation timescale,

$$t_r(r) = 0.34\sigma^3(r)/G^2 n_\star(r) M_\star^2 \log\Lambda\,, \tag{S2}$$

where $n_\star$ is the local stellar number density, the Coulomb factor is $\Lambda \simeq 0.1N_{\rm tot}$ in a single-mass cluster (*46*), and $N_{\rm tot}$ is the total number of stars in the cluster. In a realistic cluster with a spectrum of masses, the term $n_\star M_\star^2$ in the denominator is replaced by $n_\star \langle M_\star^2\rangle$, where $\langle\cdots\rangle$ denoted an average over the mass function. Since $\langle M_\star\rangle^2 \leq \langle M_\star^2\rangle$ by definition, and typical stellar mass functions have $\langle M_\star\rangle^2 \ll \langle M_\star^2\rangle$, naively substituting $M_\star$ by $\langle M_\star\rangle$ in the single mass expression (Eq. S2) may substantially over-estimate the actual relaxation time by a factor $\langle M_\star^2\rangle / \langle M_\star\rangle^2$.

The lifespan of compact clusters, such as considered here, is limited by their internal dynamics. The stars in the cluster will eventually destroy each other by physical collisions. The mean time between grazing collisions per star is

$$t_{\rm graze}^{-1} = 16\sqrt{\pi} n_\star \sigma R_\star^2 \left(1 + GM_\star/2\sigma^2 R_\star\right)\,, \tag{S3}$$

where $R_\star$ is the stellar radius. Full destruction takes multiple grazing collisions and the typical timescale is $t_{\rm coll} \sim 10 t_{\rm graze}$ (*47*). Even if the stars are able to survive collisions, the cluster will ultimately evaporate on a timescale of $t_{\rm evap} \sim 100 t_{rh}$ (*39*), where $t_{rh}$ is the relaxation time at the half mass radius $r_h$ ($r_h \simeq 1.3R_c$ for the Plummer model). For the cluster model considered here, $t_{rh} \simeq 0.9N_\star/\left[s^2\Omega_c \log(0.28N_\star)\right]$. Cluster dissolution by energetic 2-body ejections of stars is a significantly slower process, and can be neglected (*39*). The two-body ejection of the BH itself from the cluster is further suppressed by the mass ratio $1/(1+Q)$ and is therefore a low-probability event (*48*).

In addition to uncorrelated 2-body relaxation, which is inherent to any discrete system, stars in potentials with a high degree of symmetry rapidly randomize their angular momentum by the process of resonant relaxation (RR) (*40*, *41*). The central part of the cluster on length-scale $\Delta_\bullet$ is expected to be nearly spherically symmetric, which implies that the $N_\bullet \sim N_\star(\Delta_\bullet)$ background stars there will tend to conserve their orbital planes, gradually tracing rosettes. Averaged over time, the effect of the stars on the BH can be represented by the residual specific torque $\boldsymbol{\tau}$ that results from the superposed torques by $N_\bullet$ randomly oriented mass annuli, whose magnitude is $\tau = A_\tau\sqrt{N_\star(A_\star\Delta_\bullet)}GM_\star/\Delta_\bullet$, where $A_\tau$ and $A_\star$ are order unity pre-factors. This residual torque will change the orientation of the BH orbit coherently ($\propto t$), as long as the orbital planes of the background stars remain approximately fixed, over a coherence time. The longest possible coherence time is set by the mutual resonant torques between the background stars, which ultimately randomize their orbits, and hence $\boldsymbol{\tau}$, on the self-quenching coherence time $t_{\rm coh} = A_{\rm coh}J_c/\tau$, where $A_{\rm coh}$ is an order unity prefactor, and $J_c = \sqrt{GM(<\Delta_\bullet)\Delta_\bullet}$ is the circular angular momentum, with $M(<\Delta_\bullet)$ the total mass inside $\Delta_\bullet$. On timescales longer than $t_{\rm coh}$, the large change over a coherence time, $\tau t_{\rm coh}$, becomes the step-size of a random walk evolution ($\propto\sqrt{t}$). The RR timescale is then defined by $(\tau t_{\rm coh})\sqrt{t_{RR}/t_{\rm coh}} = J_c$.

For the purpose of randomizing the accretion flow's angular momentum, the relevant changes are those of the orbital orientation (direction of the angular momentum vector), and the corresponding coherence timescale is the self-quenching timescale. This restricted form of RR is

known as vector RR (*40*). The values of the numeric pre-factors for vector RR, $A_\tau$ (torque strength), $A_\star$ (size of the effective torquing volume) and $A_{\rm coh}$ (length of the coherence time), can be determined by simulations (*49*, *50*), but are poorly known at this time for the configuration of interest here (a spherical stellar system without a central massive BH). Based on the available results, we conservatively estimate

$$t_{vRR}(\Delta_\bullet) \sim 3\sqrt{\frac{M_c}{sM_\star}}\Omega_c^{-1}\left(\frac{\Delta_\bullet}{R_c}\right)^{3/2}\,, \tag{S4}$$

As in the case of 2-body relaxation, a stellar mass spectrum typically accelerates RR. For vector RR, the substitution of $M_\star$ by $\langle M_\star\rangle$ over-estimates the relaxation time by a factor of $\langle M_\star^2\rangle^{1/2}/\langle M_\star\rangle$.

The cluster potential fixes the Jeans scale for gravitational instability. Simulations (*29*, *28*) indicate that the cold flows create an isothermal cusp that is nearly pressure supported, implying that the gas mass inside the Jeans length $\lambda_J \sim \sqrt{\pi c_s^2/G\bar\rho_c}$, ($\bar\rho_c = 3M_c/4\pi R_c^3 = \bar\rho_g/(1-s)$) is close to the Jeans mass (*39*),

$$M_{g,J} \sim \frac{4\pi}{3}\left(\frac{\lambda_J}{2}\right)^3\bar\rho_g = \frac{\pi^{5/2}}{6}\frac{c_s^3}{G^{3/2}\bar\rho_c^{1/2}}(1-s)\,. \tag{S5}$$

Marginal stability then implies that the sound speed is

$$c_s^2 \simeq \frac{3}{\pi^2}V_c^2 = \frac{3}{\pi^2}\frac{GM_c}{R_c}\,. \tag{S6}$$

The accretion of non-rotating, pressure-supported gas by the BH exerts a drag force on it, $\ddot{\boldsymbol{r}}_\bullet = -(\dot M/M_\bullet)\dot{\boldsymbol{r}}_\bullet$. When the mass accretion rate rises above the 2-body relaxation rate, equipartition can no longer be maintained, and the BH dynamics can be approximately described as those of a damped 3D harmonic oscillator in the potential of the constant density core,

$$\ddot{\boldsymbol{r}}_\bullet = -2(\gamma_a+\gamma_{\rm df})\dot{\boldsymbol{r}}_\bullet - \Omega_0^2\boldsymbol{r}_\bullet\,,$$

where $\gamma_a(t) = \dot M(t)/2M_\bullet = M_\bullet(t)/2M_it_\infty$ (for the Bondi solution) is the accretion damping coefficient, and $\gamma_{\rm df}(t) = (2^{3/2}\pi^{1/2}/3)\log\Lambda G^2\rho_cM_\bullet(t)/\sigma^3$ is the dynamical friction damping coefficient (*39*). Therefore, after the BH decouples dynamically from the stellar cluster, the amplitude of the orbital oscillations decays, and since both damping coefficients scale as $\propto M_\bullet$, so does the orbital frequency.

## S2 Angular momentum in the accretion flow

A basic ingredient of this supra-exponential growth scenario is that the initial BH is a low-mass stellar BH, which is therefore scattered substantially by the random perturbations of the

cluster stars. This results in accelerated motion, which in turn induces angular momentum in the captured gas relative to the accreting BH, due to the velocity and density gradients across the capture cross-section (Figure S1; (*51*)). This occurs even though the gas in the cluster is pressure-supported, and therefore not rotating relative to the cluster center, and the stellar system, which is assumed to have formed from the gas, is not rotating as a whole relative to the gas. A necessary condition for prompt accretion is that the specific angular momentum in the captured wind, $j_a$, be lower than that of a plunge orbit, $j_{\rm ISO} = 4r_g c$ (parabolic orbit assumed). This allows the gas to flow directly into the wandering BH. Otherwise, it settles into a slowly-draining viscous accretion disk at the circularization radius $r_c \simeq j_a^2/GM_\bullet$. This constitutes an angular momentum barrier that slows down the growth of the BH (*52*).

We focus here on the early stages of the BH growth, when the BH mass is still low enough for it to wander substantially away from the center at a large fraction of the sound speed, and when its accretion radius is still much smaller than its wandering radius ($r_a \ll \Delta_\bullet$, which corresponds to $M_\bullet \ll 300\,M_\odot$ for the model of table 1), so the accretion can be described in terms of a wind. However, this regime of subsonic wind accretion, and in particular the question of angular momentum capture by motion relative to an inhomogeneous medium, is little explored and poorly understood. Analytic and numeric results on the capture efficiency of angular momentum from an inhomogeneous wind are currently available only in the ballistic (supersonic) limit (*37*, *38*). We adopt these results here and modify them to provide a rough estimate of the angular momentum accreted by the wandering BH seed. More detailed work, and in particular numeric simulations, are required for validating this analysis.

Ballistic wind accretion, which is a reasonable approximation in the hypersonic limit where gas pressure can be neglected, occurs when initially parallel flow lines in the accretion cylinder on diametrically opposed sides of the accretor, are focused behind it, intersect dissipatively by shock, cancel their transverse momentum, become bound to the accretor, and finally fall radially on the BH from the back. When the wind is homogeneous, the line of intersection is on the axis of symmetry. Davies and Pringle (*53*) showed that density or velocity gradients in a 2D (planar) flow do not change the outcome, to 1st order in the gradient: both the mass accretion rate and the zero angular momentum in it remain as they were in the homogeneous case. Instead, the intersection line curves to compensate for the imbalance in the transverse momentum, and the shocked gas then falls in radially from the point of intersection. However, Davies and Pringle noted that these results can not be directly carried over to 3D flows. The 3D case was addressed by hydrodynamic simulations. Livio, Soker and collaborators (*37*) studied flows with density gradients, and found that the mass capture rate remains close to that of homogeneous wind accretion, but the fraction of specific angular momentum that is captured is only $\eta_j \sim 0.10$–$0.25$ of that available in the accretion cylinder. Ruffert studied flows with both density (*38*) and velocity (*54*) inhomogeneities with higher resolution simulations, and found that the mass capture efficiency remains high, and the mean fraction of captured angular momentum varies with very strong dependence on the flow parameters, $\eta_j \sim 0.0$–$0.7$. We therefore adopt here a representative angular momentum capture efficiency of $\eta_j = 1/3$.

A density gradient across the capture cross-section is present when the velocity has a trans-

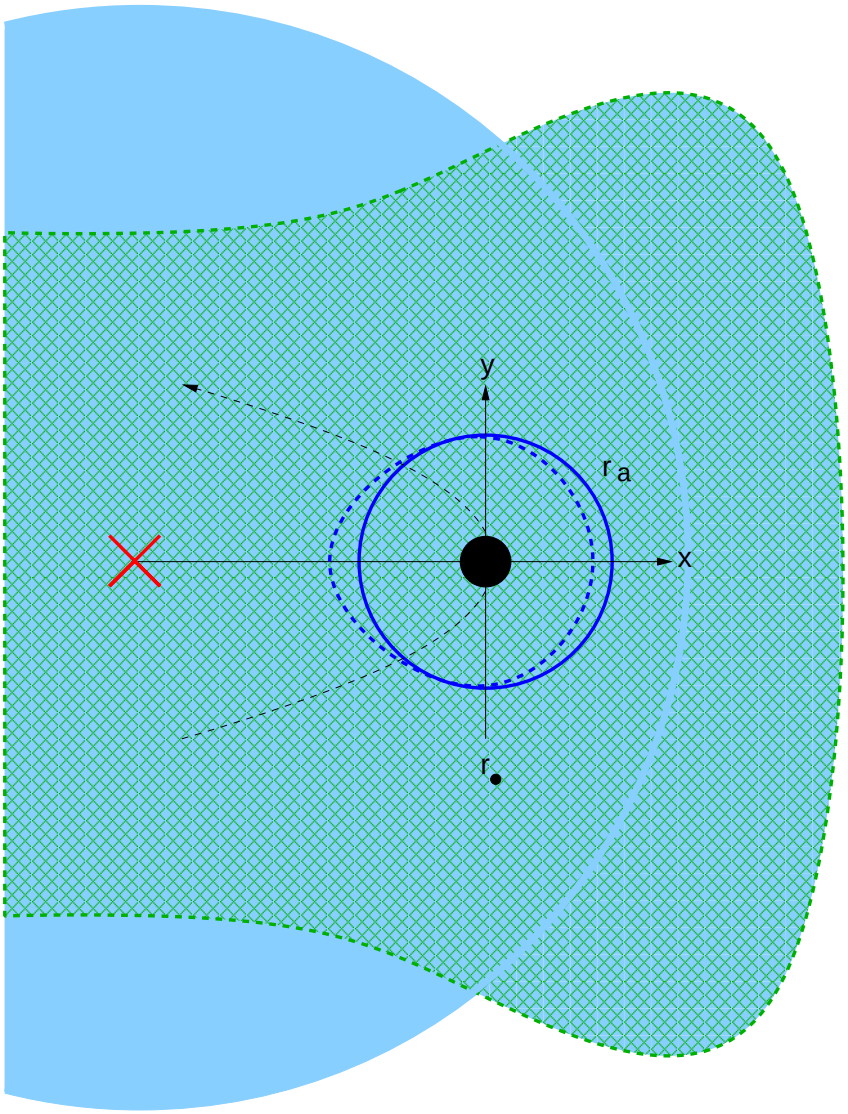


Figure S1: The geometry assumed for estimating the angular momentum of the accreted wind in the ballistic approximation. A BH (black circle) accretes from the gas reservoir (green hashed area) as it orbits (dashed arrow) at radius $r_\bullet$ around the center (red cross) of the stellar core (light blue area). The accretion cross-section of mean radius $r_a(r_\bullet)$ (dark blue circle) intercepts the flow on either side of the $y$-axis. The properties of the captured gas are asymmetric relative to the $y$-axis: the density falls with $x$ as a Plummer law, while the induced velocity $v(r_\bullet + x) = \Omega(r_\bullet)(r_\bullet + x)$ rises with $x$. The velocity gradient also skews the accretion radius (blue dashed curve). As a result, the captured gas in the accretion flow acquires angular momentum relative to the BH (see analysis in Section S2).

verse component relative to the radius vector, and an induced velocity gradient is present when the acceleration has a transverse component relative to the velocity vector. The gradients are therefore maximal on a circular orbit. For an isotropic distribution of velocities and accelerations, the rms gradients are $\sqrt{2/3}$ times smaller. Consider for simplicity a BH on a circular orbit at radius $r_\bullet$ from the cluster center, moving with velocity $v_0(r_\bullet) = \Omega(r_\bullet) r_\bullet$ relative to gas with density $\rho_0(r_\bullet)$. Denote by $x$ the location relative to the BH along the radial direction (i.e. along the gradients) in the plane of the capture cross-section, and by $y$ the location in the direction perpendicular to it and to the acceleration vector (Figure S1). A velocity gradient also affects the accretion of angular momentum by modifying the size of the accretion radius, $r_a(x) = 2GM_\bullet/[c_s^2 + v^2(r_\bullet + x)]$, thereby skewing the accretion cross-section: it is more extended where the induced velocity is smaller, on the side closer to the cluster center, and less extended on the opposite side. It is convenient to measure velocities in terms of the asymptotic sound speed, $u = v/c_s$, and distances in the $x - y$ plane in terms of the unperturbed accretion radius $r_a(0) = 2GM_\bullet/(1+u_0^2)$, so that $d_a(x) = r_a(x)/r_a(0) = (1+u_0^2)/(1+u^2(x))$. The variations in density and velocity along the $x$-axis can be described to 1st order by the dimensionless gradients $\epsilon_\rho$, $\epsilon_u$,

$$\rho(x) = \rho_0(1 + \epsilon_\rho x)\,, \qquad u(x) = u_0(1 + \epsilon_u x)\,. \tag{S7}$$

Assuming that the cluster gas is pressure-supported ($c_s^2 = (3/\pi^2)V_c^2$), the typical scale of the gradients here is $\epsilon \sim \mathcal{O}(r_a/R_c) = (2\pi^2/3)(M_\bullet/M_c) \sim 10^{-3}$.

Gas approaching the BH with impact parameters $(x, y)$ is captured when $\sqrt{x^2+y^2} < d_a(x)$. The mass capture rate through an element $\mathrm{d}x\mathrm{d}y$ of the accretion cross-section is $\mathrm{d}\dot{M}_a = \rho(x)v(x)\mathrm{d}x\mathrm{d}y$, and the angular momentum capture rate is $\mathrm{d}\dot{J}_a = \rho(x)v^2(x)x\mathrm{d}x\mathrm{d}y$. The total accretion rate through the capture cross-section is therefore (*36*)

$$\begin{aligned}
\dot{M}_a &= 2\int_{x_-(\epsilon_u)}^{x_+(\epsilon_u)} \rho(x)u(x)\sqrt{d_a^2(x) - x^2}\mathrm{d}x \simeq \pi\rho_0 u_0\,, \\
\dot{J}_a &= 2\int_{x_-(\epsilon_u)}^{x_+(\epsilon_u)} \rho(x)u^2(x)x\sqrt{d_a^2(x) - x^2}\mathrm{d}x \simeq \frac{1}{4}\left[\epsilon_\rho - 2\frac{(3u_0^2-1)}{u_0^2+1}\epsilon_u\right]\pi\rho_0 u_0^2\,,
\end{aligned} \tag{S8}$$

where the integration limits $x_- < 0$ and $x_+ > 0$ are the solutions of the cubic equation $x_\pm = \pm d_a(x_\pm)$, and the approximate expressions are to first order in $\epsilon_\rho$ and $\epsilon_u$ for finite velocities (unlike (*36*), where $u_0 \to \infty$). Converting back to dimensional units and reinstating the notation $r_a = r_a(0)$, the specific angular momentum in the accretion flow is generally

$$\begin{aligned}
j_a &= \dot{J}_a/\dot{M}_a = \frac{1}{4}\left(\epsilon_\rho - 2\left(\frac{3u_0^2-1}{u_0^2+1}\right)\epsilon_u\right) v_0 r_a \\
&= \frac{1}{4}\left(\left.\frac{\mathrm{d}\log\rho}{\mathrm{d}\log r}\right|_{r_\bullet} - 2\left(\frac{3u_0^2-1}{u_0^2+1}\right)\left.\frac{\mathrm{d}\log v}{\mathrm{d}\log r}\right|_{r_\bullet}\right)\Omega(r_\bullet)r_a^2\,.
\end{aligned} \tag{S9}$$

For the Plummer model assumed here, the dimensionless density gradient is always negative,

$$\left.\frac{\mathrm{d}\log\rho}{\mathrm{d}\log r}\right| = -5\frac{(r/R_c)^2}{(1+(r/R_c)^2)}\,. \tag{S10}$$

The induced velocity gradient across the accretion cross-section due to the accelerated motion of the BH in a non-rotating cluster is purely geometrical (the projection of the BH's angular velocity on the position of the accretion radius), $v(r_\bullet+r_a)=\Omega(r_\bullet)(r+r_a)$, so $\mathrm{d}\log v/\mathrm{d}\log r=1$. The 1st order estimate of the accreted specific angular momentum in the ballistic approximation for finite velocities, averaging of isotropic orbital velocities and accelerations and taking into account the typical accretion efficiency $\eta_j=1/3$, is therefore

$$j_a(r_\bullet)=\frac{1}{4}\sqrt{\frac{2}{3}}\eta_j\left\{\left.\frac{\mathrm{d}\log\rho}{\mathrm{d}\log r}\right|_{r_\bullet}-2\left[\frac{3(v_\phi(r_\bullet)/c_s)^2-1}{(v_\phi(r_\bullet)/c_s)^2+1}\right]\right\}\Omega(r_\bullet)r_a^2\,. \tag{S11}$$

Substituting for $r_\bullet$ the wandering radius in equipartition, $z_\bullet=\Delta_\bullet/R_c=\sqrt{2/3Q}$, so that $\mathrm{d}\log\rho/\mathrm{d}\log r=-5z_\bullet^2/(1+z_\bullet^2)$ and assuming that the gas is pressure supported, so that $(v_\phi/c_s)^2=(2^{3/2}/3)\pi^2 z_\bullet^2/(1+z_\bullet^2)^{3/2}$, fixes the mass ratio $Q$ for which $j_a=0$ to $Q_0\simeq 19.8$ in the Plummer model. With these assumptions, the value of $Q_0$ depends only on the dimensionless functional form of the potential / density pair that describes the cluster. Since typically $z_\bullet^2\ll 1$, its numeric value is not expected to depend strongly on the particular choice of the non-singular cluster potential. A BH with mass $M_\bullet\sim Q_0 M_\star$ on a typical orbit with $r_\bullet\sim\Delta_\bullet$, will therefore tend to accrete mass with little angular momentum, because the density and velocity gradients cancel each other (Figure 2). The existence of this angular momentum minimum near the initial BH mass helps suppress the accumulation angular momentum in the accretion flow in the critical initial stages of the BH seed growth.

Cluster dynamics also play such a role by randomizing the BH's orbital orientation on the short vector resonant relaxation timescale $t_{vRR}$ (see Section S1). This continually adds misaligned gas to the accretion flow, which mixes in with any gas stalled in an accretion disk, and accelerates its draining into the BH. This mechanism is particularly important at the early stages of the growth, when $M_\bullet<M_{\rm eq}=(t_\infty/t_{r0})M_i\simeq 2.5M_i$ (at $t<t_{\rm eq}=t_\infty-t_{r0}\simeq 0.6t_\infty$), before the BH can decouple from the perturbing stellar background. We derive a simple estimate of this suppression, assuming that the BH grows initially by Bondi accretion, $M(t)=M_i/(1-t/t_\infty)$, and that $j_a$ can be conservatively approximated as constant, $j_a(M_\bullet)=j_a(M_i)=j_i$, up to $M_\bullet\sim M_{\rm eq}$ (Figure 2). At these early times, the growth can be approximated as linear, $M(t)\simeq M_i(1+t/t_\infty)$. It then follows that the captured mass grows as $\Delta M=(M_i/t_\infty)t$, while the angular momentum in the flow grows in a random walk fashion as $\Delta J=[j_i(M_i/t_\infty)t_{vRR}]\sqrt{t/t_{vRR}}$ on times longer than vector RR timescale, $t_{vRR}$. The specific angular momentum accumulated in the accretion flow therefore falls with time as

$$j_a(t)=\frac{\Delta J(t)}{\Delta M(t)}\sim j_i\sqrt{\frac{t_{vRR}}{t}}\,,\quad (t>t_{vRR})\,, \tag{S12}$$

or in terms of the BH mass,

$$j_a(M_\bullet)=\frac{j_i}{\sqrt{N_{vRR}}\sqrt{1-M_i/M_\bullet}}\,,\quad (M_\bullet>\frac{M_i}{1-t_{vRR}/t_\infty})\,, \tag{S13}$$

where $N_{vRR} = t_\infty/t_{vRR}$ is the number of RR angular momentum steps over the divergence time ($\sqrt{N_{vRR}} = 7.6$ for the cluster model of table 1). Figure 2 shows that early suppression by RR decreases $j_a$ rapidly below $j_{\rm ISO}$, thereby enabling prompt radial accretion until dynamical decoupling becomes effective. This suppression of angular momentum is further aided by the angular momentum minimum near $Q_0$,

# References


44. H. Dejonghe, *MNRAS* **224**, 13 (1987).

45. P. Chatterjee, L. Hernquist, A. Loeb, *ApJ* **572**, 371 (2002).

46. M. Giersz, D. C. Heggie, *MNRAS* **268**, 257 (1994).

47. B. W. Murphy, H. N. Cohn, R. H. Durisen, *ApJ* **370**, 60 (1991).

48. D. Heggie, P. Hut, *The Gravitational Million-Body Problem: A Multidisciplinary Approach to Star Cluster Dynamics* (Cambridge University Press, 2003, 372 pp., 2003).

49. M. A. Gürkan, C. Hopman, *MNRAS* **379**, 1083 (2007).

50. E. Eilon, G. Kupi, T. Alexander, *ApJ* **698**, 641 (2009).

51. J. Frank, A. King, D. J. Raine, *Accretion Power in Astrophysics* (Cambridge University Press, 2002), third edn.

52. A. F. Illarionov, A. M. Beloborodov, *MNRAS* **323**, 159 (2001).

53. R. E. Davies, J. E. Pringle, *MNRAS* **191**, 599 (1980).

54. M. Ruffert, *A&A* **317**, 793 (1997).